Energy Levels in Na^{21}†

R. E. BENENSON* AND L. J. LIDOFSKY
Columbia University, New York, New York
(Received March 17, 1961)

The Na^{21} nucleus has been studied through two reactions: the $Ne^{20}(d,n)Na^{21}$ reaction using a fast neutron spectrometer, and the $Ne^{20}(p,\gamma)Na^{21}$ reaction using both single-crystal and Hoogenboom techniques. $\bar{E}_d$ for the neutron spectroscopy for the major part of the work was centered about 4.87 Mev, while the capturing resonance for the gamma-ray work was at $\bar{E}_p=1.17$ Mev. Enriched neon was employed as target gas.

Energy levels in Na^{21} are found at excitations of 0.33 ± 0.03 Mev, 1.77 ± 0.05 Mev, 2.42 ± 0.04 Mev, 2.80 ± 0.06 Mev, and 3.61 ± 0.06 Mev. From the neutron work level parameters can be assigned to the 0.33- and 2.42-Mev levels, while the from gamma-ray work spin limits and parity may be assigned to the 3.61-Mev level. This latter level corresponds to the 1.17-Mev capture resonance, and a study of the de-excitation cascades has been partially completed. A discussion of the level scheme of Na^{21} in terms of the collective model is given.

I. INTRODUCTION

INFORMATION about the energy-level scheme of Na^{21} has previously been obtained from a number of different experiments, but only for excitations above the proton binding energy is the information concerning the level scheme at all complete.[1] With the exception of the ground state no information on spins and parities of the low-lying levels has been available. The extension of the collective model interpretation[2] to nuclei with atomic weight just above O^{16} suggests that further information on the level structure of a nucleus such as Na^{21} is of interest, and several nuclei provide level schemes for comparison. Recent studies of the level structure of the mirror nucleus Ne^{21} provide one such scheme,[3] as do recent extensive studies[4] of Na^{23}. Collective model interpretations[2,5] predict similar rotational bands for Na^{21} and Na^{23}; the shell model also predicts a similar structure since the nuclei differ only in paired neutrons. In addition to the comparison of the Na^{21} level scheme to nuclei of nearby mass numbers, the character of the weakly bound or just unbound levels of Na^{21} could contribute some knowledge about the possibility of capture of protons by Ne^{20} in stellar reactions.

The first part of the present experiment consisted of studying the angular distribution of neutrons from the $Ne^{20}(d,n)Na^{21}$ reaction in order to observe new levels and to analyze the observed levels by stripping theory where possible. The second part of the experiment studied the gamma-ray spectrum following capture by Ne^{20} of 1.17-Mev protons. This resonance capture had been established by previous work[6,7] and corresponds to an excited state of Na^{21} at 3.61 Mev. The angular distribution of gamma rays in the direct decay to the ground state provided probable spin and parity assignments to the 3.61-Mev level, and the study of cascades through lower excited states was used to supplement the neutron spectroscopy.

II. ENERGY LEVELS OF Na^{21} FROM FAST NEUTRON SPECTROSCOPY OF THE $Ne^{20}(d,n)Na^{21}$ REACTION. EXPERIMENTAL PROCEDURES AND DATA TREATMENT

A gas recoil fast neutron spectrometer[8] was used to observe neutron groups corresponding to Na^{21} left in its excited states as a result of the $Ne^{20}(d,n)Na^{21}$ reaction. The target was neon gas enriched to 98% Ne^{20} in a thermal diffusion column.[9] For most of the neutron work, a deuteron bombarding energy of approximately 4.9 Mev was employed. The energy was set by the generating voltmeter, which had been calibrated by the $Li^7(p,n)Be^7$ reaction threshold and various higher reaction energies, and was considered known to ±20 kv. Observations were made at laboratory system angles of 0°, 20°, 45°, 60°, and 80° under five different conditions of spectrometer filling.

The principle of operation of the spectrometer permits it to cover only a portion of the neutron energy spectrum. Consequently it was necessary to change the spectrometer operating conditions in order to examine the entire energy range. Five runs were taken, two to check reproducibility since backgrounds were high. Two types of filling were employed to supply proton recoils: Research Grade propane[10] and palladium-filtered hydrogen. The first propane filling of 1.1 psi (gauge) covered the neutron energy region of 3–5 Mev. Two propane

† This work partially supported by the U. S. Atomic Energy Commission.
* Permanent address: City College, New York, New York.
[1] P. M. Endt and C. M. Braams, Revs. Modern Phys. **29**, 683 (1957).
[2] G. Rakavy, Nuclear Phys. **4**, 375 (1957).
[3] J. M. Freeman, Phys. Rev. **120**, 1436 (1960).
[4] E. B. Paul and J. H. Montagu, Nuclear Phys. **8**, 61 (1958); T. H. Kruse, R. D. Bent, and L. J. Lidofsky, Phys. Rev. **119**, 289 (1960); J. M. Freeman and J. H. Montagu, Nuclear Phys. **9**, 181 (1958/59); J. J. Singh, V. W. Davis, and R. W. Krone, Phys. Rev. **115**, 170 (1959).
[5] L. J. Lidofsky, Bull. Am. Phys. Soc. **4**, 456 (1959).
[6] K. J. Broström, T. Huus, and J. Koch, Nature **160**, 498 (1947).
[7] N. Tanner, Phys. Rev. **114**, 1060 (1959).
[8] R. E. Benenson and M. B. Shurman, Rev. Sci. Instr. **29**, 1 (1958).
[9] Through the courtesy of Professor T. I. Taylor of the Columbia University Chemistry Department.
[10] Obtained from the Matheson Company, East Rutherford, New Jersey.

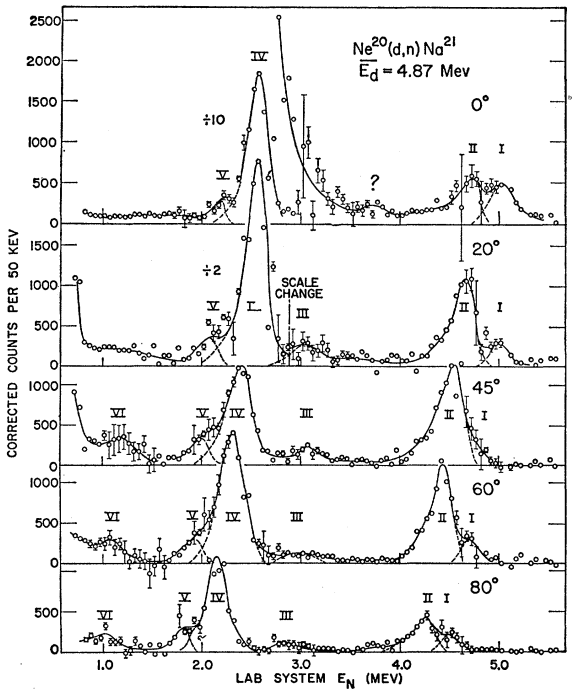

FIG. 1. Neutron spectra from the $Ne^{20}(d,n)Na^{21}$ reaction at five angles of observation. These spectra have been corrected for the change of spectrometer efficiency with neutron energy, but not for accidental anticoincidences.

fillings, one slightly below and one slightly above half-atmospheric pressure, extended the spectrum down to 2 Mev. For these latter runs the highest energy groups were still recorded but with poor efficiency. Finally, hydrogen was employed as filling in the energy region of 0.7–2 Mev. Considerable overlap of the energy regions took place from run to run permitting confirmation of spectrum features.

Neutron energy calibration in the case of two runs was provided by substituting deuterium gas in the target chamber for the Ne^{20}, lowering $\bar{E}_d$ to 1.7 Mev, and changing the angle of observation so that the individual peak positions permitted drawing a calibration curve spanning the region of interest. The peak energies were calculated from the kinematics of the $D(d,n)He^3$ reaction.[11] For three runs covering lower energy portions of the spectrum the gas used for energy calibration was CO_2, and peak positions were observed for the $C^{12}(d,n)N^{13}$, $C^{12}(d,n)N^{13*}$, $O^{16}(d,n)F^{17}$, and $O^{16}(d,n)F^{17*}$ reactions. Both bombarding energy and angle of observation were changed to provide appropriate calibration neutron energies.

A summary of the fast neutron work shown in Fig. 1 was obtained by averaging together at each angle the overlapping regions of spectra taken with different conditions. In order to perform the averaging, the individual spectra were divided into the same 50-kev intervals, and the counts per interval were averaged after two corrections were made. These corrections were (1) for changes in neutron energy due to shifts in the deuteron bombarding energy at target center from run to run, and (2) for the rapid variation of spectrometer efficiency with stopping power and protons/cm³ of the filling.

In order to make the correction for shifts in the deuteron bombarding energy for the purpose of averaging, $\bar{E}_d=4.87\pm0.02$ Mev of the first run was chosen as a basis to which subsequent bombarding energies were referred. These differed by as much as 100 kev from 4.87 Mev because of change foil thickness, target length, target pressure, and machine energy. To a very good approximation, the addition of a fixed increment to all neutron energies in a spectrum is independent of E_n; in other words, the spectrum can be shifted as a whole by an increment appropriate to the angle of observation and ΔE_d. At a given angle spectra from different runs were shifted to correspond to the same $\bar{E}_d$, and then counts per 50-kev interval were averaged with weights given by statistical error. The assumption was made that for the relatively small shifts in $\bar{E}_d$ peak heights in a spectrum would not change significantly. Before averaging the counts per interval by runs the second correction, that for variation of spectrometer efficiency with stopping power and hydrogen composition of the filling, was made according to formula (2) of reference 8.

The general features of the spectra measured at each angle but under differing conditions agreed well, but some energy intervals existed around neutron energies of 3 Mev and below 1.8 Mev, where the corrected counts did not agree even after an allowance was made for statistical and systematic errors. Backgrounds were a substantial fraction of the counting rate with neon in the gas cell. The nonreproducibility was attributed to accidental anticoincidences discussed below or impurity introduced into the hydrogen used for foil cooling when backgrounds were taken, or the accumulation of occluded gas on the foil or beam stop. Relatively small changes in background could appear as large changes in the net counts. Another possibility of error introduced in background subtraction would

TABLE I. Energy levels and level parameters of Na^{21}.

Group of Fig. 1	Q (Mev)	E_x (Mev)	l_p	J,π	θ^2
I	0.22±0.03		···	$\frac{3}{2}$+ [b]	
II	−0.08±0.03	0.33±0.03[a]	2	$(\frac{3}{2}),\frac{5}{2}$+ [c]	0.011
III	−1.55±0.05	1.77±0.05	···	···	
IV	−2.20±0.04	2.42±0.04	0	$\frac{1}{2}$+	0.21
V	−2.58±0.06	2.80±0.06	···	···	
VI	−3.39±0.06	3.61±0.06	···	$\frac{3}{2},\frac{5}{2}$+ [d]	

[a] Includes consideration of work at $\bar{E}_d=2.7$ Mev and $Ne^{20}(p,\gamma)Na^{21}$ gamma spectra.
[b] From reference 1.
[c] Value in parentheses expected unlikely from nuclear models.
[d] From angular distribution of gamma rays following $Ne^{20}(p,\gamma)Na^{21}$.

[11] J. L. Fowler and J. E. Brolley, Revs. Modern Phys. 28, 103 (1956).

appear as a result of slight differences in $\bar{E}_d$ when bombarding the principal source of background and when bombarding the neon gas.

The averaging of corrected counts per 50-kev interval for Fig. 1 was carried out by weighing the contribution according to the statistical uncertainty. This technique was chosen as being perhaps the most objective and simplest of application. The nonreproducibility referred to in the preceding paragraph was permitted to influence the assigned errors as discussed below. The averaging according to statistical weight for a given region of overlap favors the run taken with greatest spectrometer gas filling stopping power, hence, efficiency. For a given spectrum, the lowest energy of neutrons included in the averaging was determined by the recoil range of a forward-scattered proton to be about 7 cm. Such a range corresponds to the merging of the peak created by the collimation of nearly forward recoils with the spectrum of large-angle recoils which are also accepted by the collimation scheme.[8] For lower energy neutrons formula (2) of reference 8 is expected to be invalid.

The error bars shown in Fig. 1 in selected 50-kev intervals are the larger of the usual internal or external error. Since it was convenient to analyze individual runs in intervals slightly larger than 50 kev, a given run did not contribute to all adjacent intervals. For some intervals only one contribution was present; in such a case only the interval statistical uncertainty is shown. The few very large error bars in Fig. 1 arise from this latter situation when the sole contribution was from a run at low efficiency.

While the general features of the angular distribution of neutrons corresponding to Na^{21} states can be inferred from Fig. 1, the data shown have not been corrected for loss in spectrometer efficiency as a result of accidental anticoincidences. The loss in efficiency affects all portions of the spectrum at a given angle equally, but the loss changes with over-all count rate and, hence, angle of observation. The loss is highest at small angles due to the very high flux of group IV. At the time these data were taken the importance of accidental anticoincidences in affecting the spectrometer efficiency was not realized, since previous tests with monoenergetic neutrons did not reveal a marked count rate dependence. Later tests with complex spectra did indicate the necessity of such a correction. The correction is easily made by inserting pulser signals into the central counter preamplifier under run conditions. The loss in efficiency could probably be minimized by use of an amplifier having fast recovery characteristics[12] with the spectrometer outer volume counters.

Table I lists the Q values of the observed levels from the $Ne^{20}(d,n)Na^{21}$ reaction and the corresponding excitation energies of Na^{21} as derived from Fig. 1, except where noted. Individual Q values for each level were calculated from the corresponding peak energy at each angle where the peak was discernible.

[12] E. Fairstein, Rev. Sci. Instr. **27**, 475 (1956).

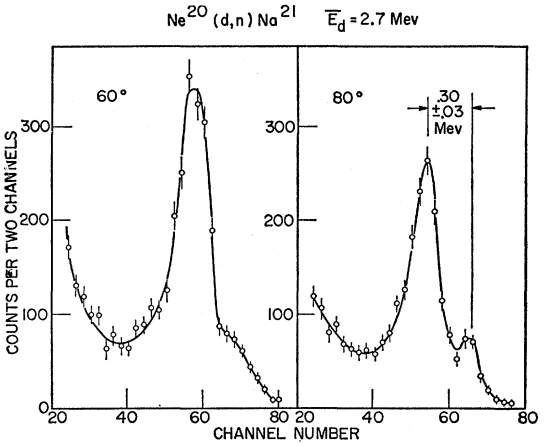

FIG. 2. Spectra from the $Ne^{20}(d,n)Na^{21}$ reaction at $\bar{E}_d=2.7$ Mev.

The estimated errors in Q values and excitation energies listed in Table I arose through (1) uncertainty in $\bar{E}_d$, (2) the subdivision of counts into 50-kev intervals, (3) uncertainty in locating the peak corresponding to a particular level, and (4) errors in calibration. Upper limits of these uncertainties were estimated to be, respectively, (1) ± 20 kev, (2) ± 25 kev, (3) between ± 25 and ± 50 kev, (4) ± 50 kev.

Since the groups labeled I and II were not clearly resolved, an attempt was made to resolve them better by lowering the generator energy to 3 Mev in order to increase the relative separation to peak energy. The results at two angles are shown in Fig. 2. The target thickness was left too great for best resolution, an estimated value of almost 200 kev, but two peaks are clearly discernible in the right side of Fig. 2. The 3-Mev data were repeated at 0°, 20°, and 45°, and the excitation energy for the first excited state from these measurements has been included in the value quoted in Table I.

In order to search for unknown levels between the state at 3.61-Mev excitation and those known from the elastic scattering of protons[1] by Ne^{20} but to take advantage of a calibrated spectrometer filling, the generator energy was raised to 5.8 Mev. The results are shown in Fig. 3, with arrows pointing to calculated positions of the levels known from proton elastic scattering. The peak and edge at 0° and 20° are considered to correspond to the known virtual levels of Na^{21} at 4.18- and 4.31-Mev excitation. The mismatch with the calculated position may be due either to the necessity of extrapolating the calibration curve or to the fact that the generating voltmeter becomes increasingly inaccurate as the generator voltage is increased. In any case, no new levels in the excitation energy region between 3.61 and 4.18 Mev appear corresponding to peaks in the 5.8 Mev data. The continuous spectrum in Fig. 3 is possibly due to three-body breakup from the $Ne^{20}(d,pn)Ne^{20}$ reaction.

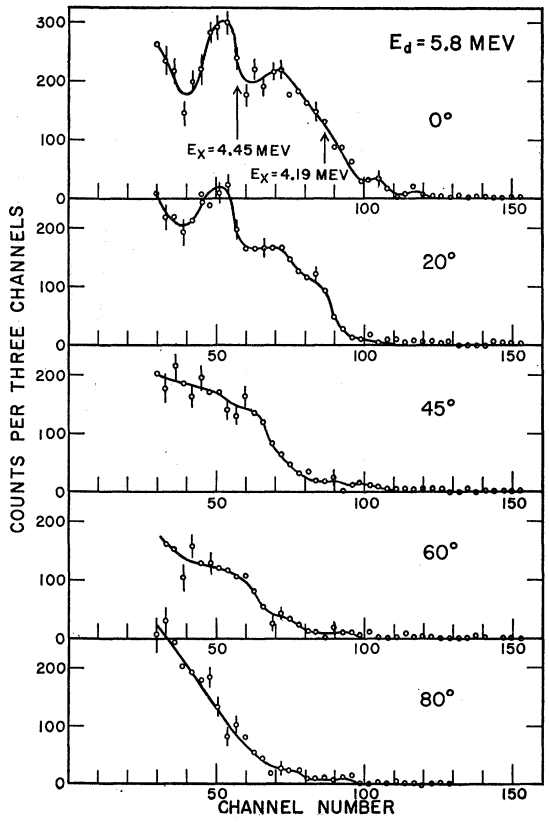

FIG. 3. Search for levels in Na^{21} having excitation energies above 3.6 Mev. The arrows indicate calculated positions of levels known from previous work.

III. DISCUSSION OF THE ENERGY LEVELS OF Na^{21}

The neutron groups which leave Na^{21} in its ground state are not clearly resolved from those which leave the nucleus in its first excited state. The good agreement in Table I with the published Q value for the reaction must be considered fortuitous.

The 0.33-Mev level corresponding to group II in Fig. 1 was previously observed by Swann and Mandeville[13] as a single peak in a neutron spectrum corresponding to a lower neutron energy than expected from the ground-state Q value of this reaction. This Q value was known from the end point of the Na^{21} positron spectrum and the nuclear mass of Ne^{21}. Swann and Mandeville correctly surmised that they were observing a transition to an excited state of Na^{21}. When the present work was first reported, this level was listed at 0.4-Mev excitation,[14] and since at 0.37 ± 0.05 Mev.[15]

The small peak in the 0° spectrum of Fig. 1 marked with a question mark would probably be ignored except that in an angular distribution taken at $\bar{E}_d=4.5$ Mev, to be discussed shortly, a small peak again appeared at 0°. The excitation energy of this level, were it in Na^{21}, would be approximately 1.3 Mev, but it possibly is associated with the residual 2% Ne^{22} in the target gas. A level at this excitation is not listed because it only appears in 0° data and has no known counterpart in Ne^{21} levels.[3]

Much of the repetition of runs discussed above was in an effort to observe again, and obtain an angular distribution of neutrons from, the 1.47-Mev level previously reported.[16] No evidence for this level can be claimed from Fig. 1. Two possibilities exist for the present failure to observed the 1.47-Mev level: Either the J value is high, inhibiting its excitation by deuteron stripping and is more easily observed by neutron threshold measurements; or else, since the previous workers were using a natural neon target, they observed a threshold in $Ne^{22}(d,n)Na^{23}$.

The 1.77-Mev level in the present work is considered to be the counterpart of the Ne^{21} 1.75-Mev level. During the course of the experiment the possibility was considered that this group was due to oxygen contamination of the neon gas. Neutrons from the $O^{16}(d,n)F^{17}$ reaction have similar energies, and except for the obscured 0° point the neutrons from the 1.77-Mev level could have a similar $l_p=2$ angular distribution.[17] The energy of the neutrons from the 177-Mev level tends to vary more slowly with angle than would be the case from $O^{16}(d,n)F^{17}$, and mass spectrographic analysis of the neon failed to reveal the presence of appreciable oxygen contamination. The gamma-ray work to be discussed below appears to confirm the presence of this level.

The 2.4-Mev level listed in Table I has been previously observed by neutron threshold measurements[16] and listed at an excitation in Na^{21} of 2.43 Mev. The extremely strong forward yield of neutrons which leave Na^{21} in this level is a striking feature of the 0° spectrum.

The 2.80-Mev level has not been previously observed but is considered to be the counterpart of the Ne^{21} 2.87-Mev state.[3] This Na^{21} state is virtual for proton emission.

The 3.61-Mev level is the one corresponding to the 1.17-Mev $Ne^{20}(p,\gamma)Na^{21}$ resonance and has been studied through its gamma emission as discussed below.

IV. ANGULAR DISTRIBUTIONS AND REDUCED WIDTHS FROM STRIPPING THEORY

Two levels in Na^{21} have proved amenable to analysis by stripping theory: values of l_p the angular momentum of the proton captured by Ne^{20} of two and zero, respectively, can be assigned to the 0.33- and 2.4-Mev levels. These assignments require that both levels have even parity, with $J=\frac{3}{2}$ or $\frac{5}{2}$ for the 0.33-Mev level, and

[13] C. P. Swann and C. E. Mandeville, Phys. Rev. **87**, 215(A) (1952).
[14] R. E. Benenson and L. J. Lidofsky, Bull. Am. Phys. Soc. **3**, 381 (1958).
[15] F. Ajzenberg-Selove, L. Cranberg, and F. S. Dietrich, Bull. Am. Phys. Soc. **5**, 493 (1960).
[16] J. B. Marion, J. C. Slattery, and R. A. Chapman, Phys. Rev. **103**, 676 (1956).
[17] F. Ajzenberg, Phys. Rev. **83**, 693 (1951).

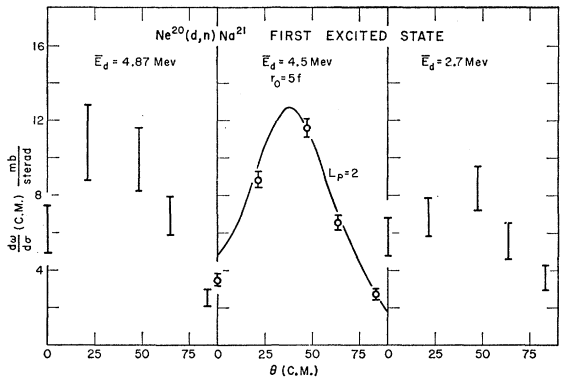

FIG. 4. Angular distributions of neutrons which leave Na^{21} in its first excited state (Group II of Fig. 1). The error bars in the left and right diagrams are drawn from consideration of uncertainty in two efficiency corrections. Error bars in the center graph are standard deviation in the number of counts. The ordinate scale uncertainty of the center graph is estimated to be $\pm 10\%$, although error in relative differential cross sections is less.

$J=\frac{1}{2}$ for the 2.4-Mev level. Both shell and collective models strongly favor the $\frac{5}{2}$ assignment for the 0.33-Mev level.

The current interest in reduced widths of levels from stripping angular distributions[18] emphasizes the necessity of measurement of absolute differential cross sections. To some extent the fast neutron spectrometer can be used to measure absolute differential cross sections through knowledge of the solid angle of acceptance of the collimated recoils, the n-p total cross section, and the range–energy relation for the filling gas. However, the accuracy of the measurement suffers in that the solid angle for acceptance of collimated recoils depends sensitively on the effective diameter of the central counter, which in turn varies slowly with outer volume gas multiplication. A preferable method of measurement of an unknown differential cross section is to calibrate the spectrometer efficiency under a given set of operating conditions using neutrons from a reaction of known cross section having nearly the same energy. Counting rates from the two reactions can be compared and differences in spectrometer efficiency from small differences in energy corrected by formula (2) of reference 8. By far the most convenient calibration reaction is the $D(d,n)He^3$ reaction.[11]

Two difficulties are encountered in attempting to assign differential cross sections from the data of Fig. 1. The first is the aforementioned lack of direct information on loss of efficiency due to accidental anticoincidences. The second was that in order to match neutron energies from the calibrating reaction with those corresponding to group IV of Fig. 1, the high Q of the $D(d,n)He^3$ reaction required that it be observed at lower $\bar{E}_d$. Calibrating spectra had to be observed at large angles of observation where counting rates were low and uncertainty in energy was very sensitive to uncertainty in angle measurement. The error in count rate at given E_n is considered to exceed 10%. The ratio of differential cross sections of the $D(d,n)He^3$ reaction calculated from the spectrometer geometry to listed values by a factor of 0.74.

In order to estimate the systematic error introduced by the loss in efficiency through accidental anticoincidences, another run was performed well after the time the data of Fig. 1 were taken. However, the value of $\bar{E}_d$ for that run was inadvertently set at 4.50 ± 0.05 Mev rather than 4.87 Mev, a fact discovered after the run and ascribable to an erroneous reading by the generating voltmeter. Several independent pieces of evidence support the conclusion of the lower bombarding energy despite the fact that the evidence is not direct. In particular, the relative separation of the peaks of the 0.33- and 2.4-Mev levels is a sensitive test of bombarding energy.

The three graphs of Fig. 4 represent the 0.33-Mev level angular distributions at three bombarding energies. The error bars for the left-hand graph, that for $\bar{E}_d=4.87$ Mev, are appreciably larger than from counting statistics alone and have been drawn after evaluation of the limits of uncertainty of the systematic errors discussed just above. Despite the large uncertainties, the shape of the angular distribution is clearly $l_p=2$. The central graph of Fig. 4 is for the $\bar{E}_d=4.5$-Mev data, and the error bars are purely from counting statistics. The fit is very good to the $l_p=2$ theoretical angular distribution calculated from the tables of Lubitz[19] using an $r_0=5.0$ f. Calibrations and correction for accidental anticoincidences were performed carefully; the error in the absolute ordinate scale is estimated at about 10%. The right-hand graph of Fig. 4 is introduced mainly to show that the cross section is somewhat smaller at $\bar{E}_d=2.7$ Mev; neutrons at forward angles seem more accentuated relative to the peak. The same remarks about error bars apply as for the left-hand graph.

The angular distribution for neutrons leaving Na^{21} in its 2.4-Mev level is shown in Fig. 5. Again the error bars represent the estimated uncertainty in systematic errors, since these are expected to be much larger than those from counting statistics. A run intended to reproduce conditions as nearly as possible was taken subsequent to that for the Fig. 1 data also to estimate accidental anticoincidence losses in the original data. The stripping angular distribution is clearly well fitted by $l_p=0$ requiring this state to be $J=\frac{1}{2}$ with even parity. The extremely large cross section at 0° is notable.

Values of θ^2, the dimensionless reduced width, were calculated from formula (II.29) of reference 18 for both the 0.33- and 2.4-Mev levels, and these values are listed in Table I. The reduced width γ^2 for the 2.4-Mev level is estimated at 0.56 Mev. Since the angular distribution for the 2.4-Mev level is fairly well fit by the theoretical curve, θ^2 was calculated without use of

[18] M. H. Macfarlane and J. B. French, Revs. Modern Phys. 32, 567 (1960).

[19] C. R. Lubitz, University of Michigan Report, 1957 (unpublished).

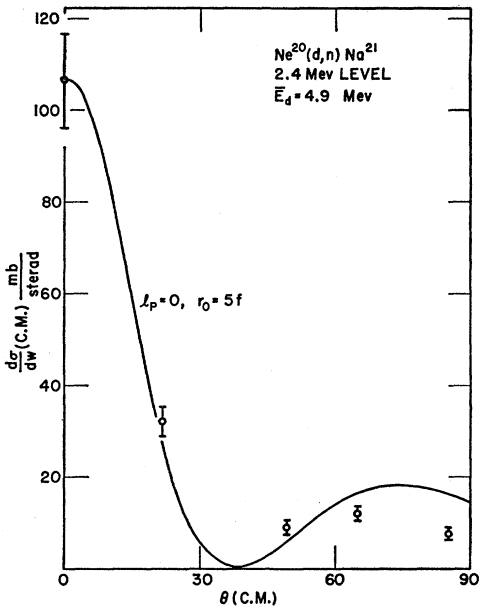

FIG. 5. Angular distribution of neutrons which leave Na^{21} in its 2.4-Mev level (Group IV of Fig. 9). Error bars are estimated from uncertainties in systematic errors.

the revision discussed in reference 18 for nearly unbound levels.

The 0° neutron group of the 1.77-Mev level is obscured by the edge of the 2.4-Mev level peak, so that an attempt to assign an l_p value would be unreliable. The differential cross sections at 20° and 45° are approximately 2 mb/sr. The large 0° cross section for the 2.4-Mev level and its unambiguous assignment suggest that if this level de-excites through a cascade involving the 1.77-Mev level a $(d,n\gamma)$ angular correlation measurement would be feasible and could successfully supply information on the latter.

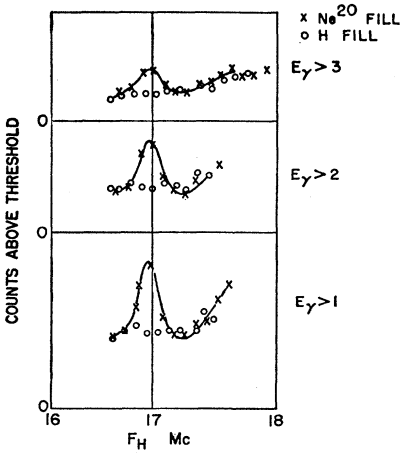

FIG. 6. The appearance of the 1.17-Mev resonance, $E_p \approx 4.25\times10^{-3} f^2$, f in Mc/sec.

V. GAMMA RAYS FOLLOWING PROTON CAPTURE IN THE $Ne^{20}(p,\gamma)Na^{21}$ 1.17-MEV RESONANCE

In the second phase of this study of Na^{21} levels, protons were substituted for deuterons in the bombardment of the Ne^{20} gas targets. Na^{21} is excited in its 3.61-Mev level when Ne^{20} captures protons in the $\bar{E}_p = 1.17$-Mev $Ne^{20}(p,\gamma)Na^{21}$ resonance.[5] In order to learn something of the character of the 3.61-Mev level since it was not amenable to analysis by stripping theory, and in order to observe possible cascades through the reported 1.47-Mev level, the 1.17-Mev resonance was relocated. The capture radiation was observed in a single 3×3 NaI crystal, and Fig. 6 shows the variation of counting rates with the field of the Van de Graaff generator analyzing magnet, as measured by the proton nuclear magnetic resonance frequency. Three discriminators measured counting rates of gamma rays above, respectively, 1, 2, and 3 Mev.

Figure 7 shows the characteristic gamma-ray spec-

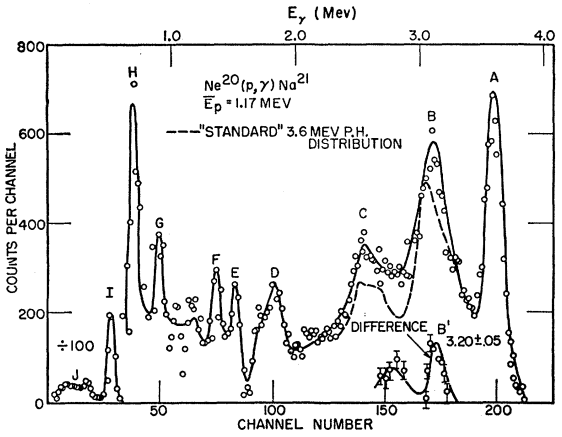

FIG. 7. Single 3×3 NaI crystal spectrum of gamma rays following capture of 1.17-Mev protons by Ne^{20}.

trum observed at the 1.17-Mev resonance; after calibrating with standard sources, the highest energy peak corresponds well to $E_\gamma = 3.6$ Mev. Background was subtracted by substituting hydrogen for the neon in the gas cell; the peaks which are labeled *H*, *G*, *E*, *D*, *C*, *B*, and *A* correspond, respectively, to gamma-ray energies of 0.7, 1.0, 1.4(5), 1.8(4) Mev, and the one- and two-escape peaks associated with the 3.61-Mev peak. However, the peaks *F* and *E* appear separately only after the subtraction of a large background, and at least one is due to $Ne^{22}(p,\gamma)Na^{23}$, as was verified on a different occasion by substituting natural for enriched neon in the target chamber. The peak *E* is favored as belonging to an Na^{21} transition between the 1.77- and 0.33-Mev levels. The small peak labeled 3.20±0.05 Mev in Fig. 7 is the result of subtracting a monoenergetic 3.6-Mev spectrum[20] from the observed spectrum. A 3.20±0.05

[20] R. L. Heath, Atomic Energy Commission Report IDO-16408, 1957 (unpublished).

Mev gamma ray would correspond to a decay from the 3.61-Mev level to the first excited state of Na^{21}.

An angular distribution of the gamma rays corresponding to the highest energy peak of Fig. 7 was obtained by rotating the same crystal around the beam axis. The experimental points of the angular distribution are shown in Fig. 8, with a least-squares fit to the points shown by the curve. In order to preserve the enriched neon, approximate background counting rates were taken by changing the proton energy to be off-resonance; this appeared justified in view of the smallness of background at the highest energy peak position.

The curve through the experimental angular distribution of Fig. 7 was fitted using the formulas and tables of Sharp, Kennedy, Sears, and Hoyle.[21] The best fit was obtained by giving the 3.61-Mev level a $\frac{3}{2}^+$ assignment, but the possibility of a $\frac{5}{2}^+$ assignment also existed.

Attempts to observe single-crystal spectra by exciting Na^{21} through higher $Ne^{20}+p$ resonances led only to spectra identifiable as coming from de-excitation gamma rays of the $Ne^{20}(p,p')Ne^{20*}$ and $Ne^{22}(p,p')Ne^{22*}$reactions.

Following the above work a search was made for gamma-ray transitions in cascade from the 3.61-Mev level using the recently described Hoogenboom technique.[22]

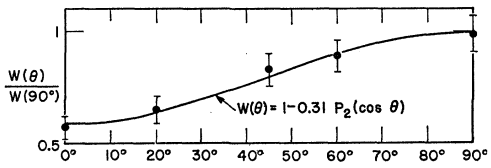

FIG. 8. Angular distribution of gamma rays corresponding to peak A of Fig. 7.

The Hoogenboom technique involves the use of two scintillation crystal spectrometers whose over-all gains are carefully matched to be equal for equal gamma-ray energies. The two scintillation crystals are usually arranged on opposite sides of the target chamber. A signal from one of the two crystals is recorded, but only when the sum of the signals from both matched detectors adds up to the pulse height corresponding to the full energy of the direct capturing level-to-ground-state transition. For this purpose, a linear adder circuit sums the signals from the two crystals and sends the sum signal into a single-channel analyzer used to gate the multichannel analyzer recording the one-crystal output. The great advantage of the technique is that gamma rays must correspond to cascades or direct transition from only one capturing level, and furthermore, only peaks corresponding to the full energy of the cascade gamma rays will be recorded. One- or two-escape peaks or Compton edges are almost completely eliminated.

[21] W. T. Sharp, J. M. Kennedy, B. J. Sears, and M. G. Hoyle, Atomic Energy Canada Limited Report AECL-97 or CRT-556, rev. 1954 (unpublished).

[22] A. M. Hoogenboom, Nuclear Instr. 3, 57 (1958).

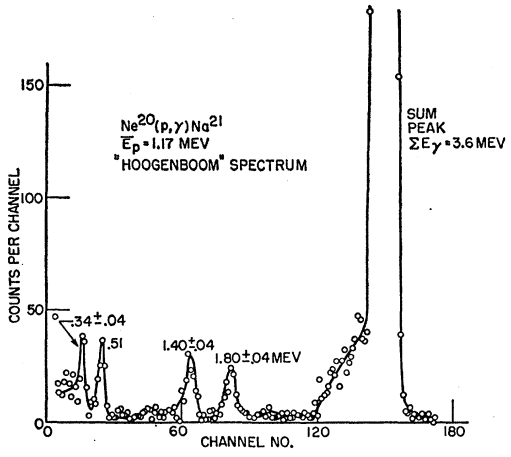

FIG. 9. Spectrum of gamma rays observed using the Hoogenboom technique. Sum channel set to correspond to group A of Fig. 7.

A typical Hoogenboom spectrum following proton capture by the 3.67-Mev level in Na^{21} is shown in Fig. 9: A 0.51-Mev peak, three small peaks, and a vastly larger peak corresponding to the direct ground-state transition appear. This spectrum reproduced very well on two separate occasions; the energies of the three small peaks are respectively 0.34, 1.42, and 1.83 Mev. The estimated uncertainties are ±0.04 Mev, largely

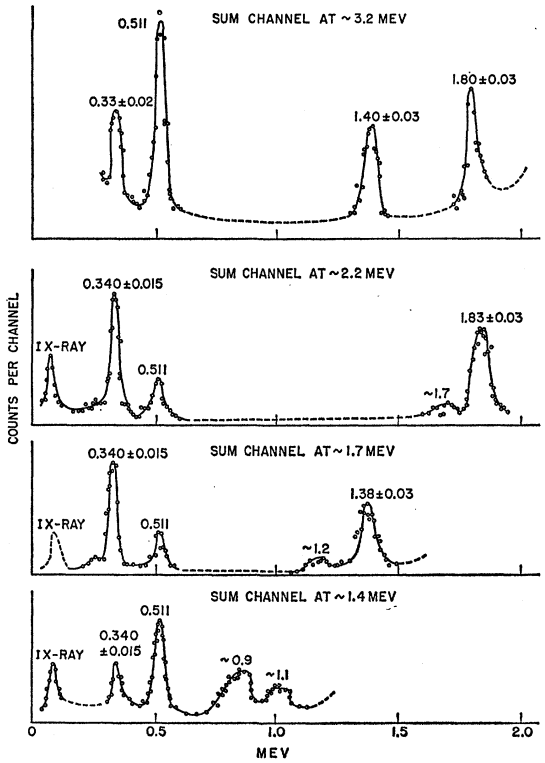

FIG. 10. Spectra of gamma rays observed using the Hoogenboom technique but setting the sum channel at energies other than shown in Fig. 9.

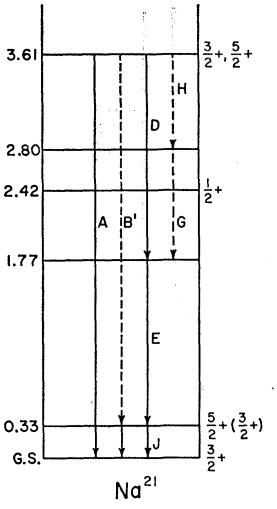

FIG. 11. Energy-level scheme of Na^{21} from present work. Gamma-ray transitions are labeled by letters corresponding to peaks in Fig. 7. Dashed lines indicate transitions based purely on energy differences with no further supporting evidence.

due to error in calibration. Since the photomultiplier tubes exhibited gain drift with source strength, making the use of standard sources difficult, calibration curves were mostly obtained from the 0.51- and 3.61-Mev points.

At first glance it would appear that the 1.42-Mev gamma ray might correspond to the 1.47-Mev level previously reported[16] but not observed now in the (d,n) investigation. That the 1.82-Mev gamma-ray peak has very nearly the same area as the 1.42-Mev peak in Fig. 9 suggested that it is in coincidence with the 1.42-Mev gamma ray according to the requirements of the Hoogenboom technique. However, the sum of the two energies does not add up to 3.61 Mev, and the extreme smallness of the two peaks compared to the direct ground-state transition is striking when compared to spectra shown in Hoogenboom's article. If, however, the 0.34-Mev gamma-ray energy is added to the other two, the sum is very nearly 3.61 Mev. Such a result suggests that a triple coincidence is involved: Two gamma rays are captured by one crystal when one is captured by the other. A three-gamma cascade would negate the identification of the 1.42-Mev gamma ray with the 1.47-Mev level.

In all probability the 1.42- and 1.82-Mev gamma rays are captured in opposite crystals. Simultaneously one crystal captures either a 0.34-Mev photon or one of many low-energy gamma rays in an accidental coincidence such that the summed energies fall within the relatively wide single-channel analyzer window. To help check this interpretation, the sum channel after the linear adder was set for 1.82+0.34 Mev to see if just two peaks would appear, and set for 1.42+0.34 Mev for the same reason. In both cases the two peaks appeared, one being the 0.34-Mev peak; and when the sum channel was set at a figure not a sum, the peaks were attenuated. They did not disappear completely, since Compton-effect electron energies in one crystal could now be added to a full-energy peak in the other and satisfy a sum requirement set below the full excitation energy of the capture level. The results of this last investigation are shown in Fig. 10.

In order to dismiss the possibility that what was being observed was the de-excitation of Ne^{21} following a possible β^+ decay to its 1.74-Mev level along with simultaneous observation of annihilation quanta, note must be taken of a previous experiment[23] where no gamma rays were found of energy greater than 0.51 Mev following the positron decay of Na^{21}. Furthermore, the observed energies in the present experiment do not quite agree with those expected for Ne^{21} de-excitation, and no explanation could be given then for the Hoogenboom spectrum.

The interpretation of the gamma-ray decay scheme to bring it into consistency with the level scheme from the (d,n) work is that alternatively to a strong direct ground-state transition, the 3.61-Mev level de-excites through the 1.77-Mev level, and this latter through the 0.33-Mev level.

A level scheme for Na^{21} showing the observed levels and present interpretations of the gamma-ray cascades is shown in Fig. 11. An attempt has been made to label some of the transitions to be consistent with the peaks of Fig. 7.

VI. COMPARISON WITH COLLECTIVE MODEL

The successful description of the structure of F^{19} and $Al^{25}-Mg^{25}$ by means of a collective model strongly suggests that a similar model might well describe the structure of sodium isotopes. However, an inspection of the Nilsson[24] diagrams shows that the description of an odd-A nucleus with an odd group consisting of 11 nucleons (Na^{21}) will be considerably more complex than that for 13 odd nucleons ($Al^{25}-Mg^{25}$) or for 9 (F^{19}) because of rotation-particle coupling (RPC).[25] This

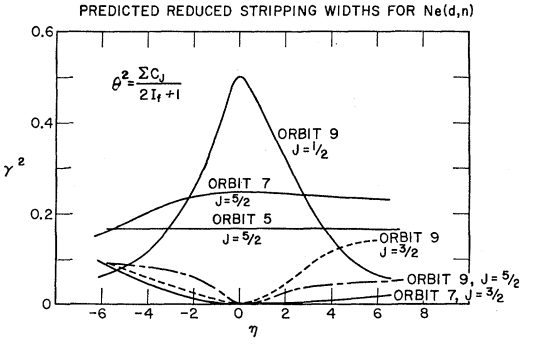

FIG. 12. Predicted reduced widths for the $Ne^{20}(d,n)$ reaction according to the collective model.

[23] G. E. Schrank and J. R. Richardson, Phys. Rev. **86**, 248 (1952); W. L. Talbert, Jr., M. G. Stewart, and D. J. Zaffarano, Bull. Am. Phys. Soc. **5**, 10 (1960).

[24] S. G. Nilsson, Kgl. Danske Videnskab. Selskab, Mat.-fys. Medd. **29**, 16 (1955).

[25] A. K. Kerman, Kgl. Danske Videnskab. Selskab, Mat.-fys. Medd. **30**, 15 (1956).

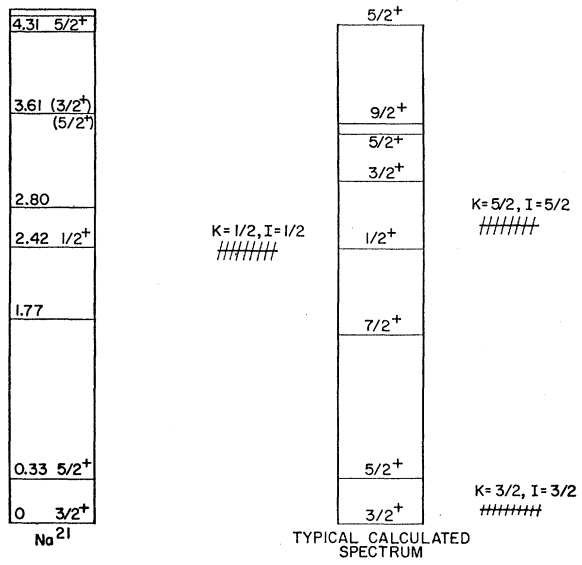

FIG. 13. Positive-parity states in Na^{21}.

interaction couples together states of a given J originating from bands of K_1 and K_2 if $K_1-K_2=\pm 1$ and strongly perturbs the simple rotational scheme. For 13 nucleons, the lowest bands have $K=\frac{1}{2}$, $K=\frac{5}{2}$, $K=\frac{1}{2}$ so that RPC does not take place; for 9 nucleons the lowest bands have $K=\frac{1}{2}$ and $K=\frac{3}{2}$ so that only one RPC matrix element is effective. However, for 11 nucleons the bands are $K=\frac{3}{2}$, $K=\frac{1}{2}$, $K=\frac{5}{2}$, so that two RPC matrix elements contribute. The number of parameters involved is such that the description is not completely determined. Despite these difficulties, certain properties of Na^{21} and reactions involving Na^{21} which are in accord with the general predictions of the model can be described.

(a) Among the static properties of Na^{21}, both its ground-state spin, $\frac{3}{2}$, and the positive quadrupole moment of its mirror nucleus[26] Ne^{21} are in accord with a description of its ground state as nearly pure $K=\frac{3}{2}$, $J=\frac{3}{2}$ with positive deformation $\eta\sim 4$.

(b) A calculation of single-particle widths can be made for the various states of a rotational nucleus. The calculation leads to the general expression for the reduced width for stripping[27]:

$$\theta^2/\theta_0^2=[2(2J_i+1)/(2J_f+1)]\sum_j|C_j|^2(J_i j K_i\Omega|J_f K_f)^2,$$

where (J_i,K_i) and (J_f,K_f) are the initial and final nuclear angular momentum and projection along the symmetry axis, respectively, where $(j\Omega)$ is the same for the added nucleon, θ^2 is the reduced width for the state, and θ_0^2 is the single-particle reduced width. Specifically, for $Ne^{20}(d,n)$, after setting $\theta_0^2=1$,

$$\theta^2=[2/(2J_f+1)]|C_{Jf}|^2.$$

θ^2 is plotted for several states in Fig. 12. The orbit numbers are those of Nilsson.[24] Several features are to be noted. The $j=\frac{1}{2}$ state of Na^{21} is expected to be pure $K=\frac{1}{2}$. The measured $\theta^2=0.21$ for $Ne^{20}(d,n)$ to that state then corresponds to η between 3 and 4. The ground and first excited states of Na^{21} are expected to have large components of $K=\frac{3}{2}$, $j=\frac{3}{2}$, and $j=\frac{5}{2}$, respectively. Although the measured $\theta^2=0.011$ is small compared to the predicted values, the model does predict a much larger cross section for $Ne^{20}(d,n)$ to the $\frac{5}{2}^+$ state than to the $\frac{3}{2}^+$ state, in agreement with experiment.

These same stripping data could also be described in terms of the shell model. The large cross sections to the $\frac{1}{2}^+$ state would correspond to the fact that the $2s_{\frac{1}{2}}$ state is essentially unfilled. The cross section to the $\frac{5}{2}^+$ state would be somewhat reduced because the $1d_{\frac{5}{2}}$ shell is partially filled. Finally, the ground state would not be a single-particle state and would have a very small cross section.

(c) Although the large number of available parameters precludes the possibility of a detailed fit, reasonable fits to the level scheme were made of which a typical one is illustrated in Fig. 13. The procedure followed was to (1) select a distortion which was chosen to be the same for all bands, (2) calculate the RPC matrix element and decoupling parameter, (3) fit the $K=\frac{1}{2}$ intrinsic state to be the observed $j=\frac{1}{2}^+$ state, and (4) select moments of inertia for the other bands and positions for their intrinsic states to generate the observed spacing of the $\frac{1}{2}^+$ state above the ground state and to reproduce the general positions of the other states as well as possible. For all fits attempted, it was found necessary to constrain the intrinsic state positions to the excitations noted by the cross-hatched areas of of Fig. 13. In addition, the distortion parameters were held to the range $\eta=3$–6, and moments of inertia were held to be of an order consistent with the position of the first excited states of Ne^{20} and Mg^{24}. It should be noted that the order of states just above the $\frac{1}{2}^+$ state is very sensitive to the exact parameters chosen, and so is not well represented by a "typical" fit.

ACKNOWLEDGMENTS

The authors would like to express their thanks to Professor T. I. Taylor for the use of the thermal diffusion column and advice on its operation, to Vincent Saltamach for analysis of the neon, and to Richard Heitler for assistance with the calculations.

[26] G. M. Grosof, P. Buck, W. Lichten, and I. I. Rabi, Phys. Rev. Letters **1**, 214 (1958).
[27] A. E. Litherland, H. McManus, E. B. Paul, D. A. Bromley, and H. E. Gove, Can. J. Phys. **36**, 378 (1958).